Proceedings of ERAD (2004): 278–280 © Copernicus GmbH 2004

ERAD 2004

Retrieving ice precipitation using a radar snow profiling algorithm

E. Moreau, J. Testud, and E. Le Bouar

Novimet, 10–12 av. de l'Europe 78140 Vélizy, France

Abstract. Retrieving ice precipitation from radar reflectivity is subject to large uncertainties, due to the variability of the standard Z-R relationship in the ice phase. In this paper, a new algorithm (called hereafter SPA) is proposed for retrieving ice precipitation associated to stratiform clouds, using the vertical profile of reflectivity Z. This algorithm is based on a simplified model of ice particle aggregation. SPA is a profiling algorithm since it helps to invert the vertical profile of Z to deliver the corresponding profiles of various physical parameters of interest: the mean volume diameter (D_m), the intercept parameter N_o*, the ice water content *IWC* and the precipitation rate R.

A first validation of SPA is presented using vertical profiles of reflectivity from a ground based UHF radar, and drop size distributions measured by a collocated POSS instrument.

1 Introduction

The limitation of standard $Z - R$relationship for ice lays in the implicit assumption that at the whole profile of reflectivity is attached a single value of N_0^*. We know that this is incorrect. For example, at the top of an ice precipitation layer, the low reflectivity is generally produced by a number of very small particles (pristine ice) that had no time yet to aggregate. N_0^* in such circumstances may be of the order of 10^{11} to 10^{12} m^{-4}. At the base of the same cloud, a low reflectivity may be the result of evaporation of a moderate number of big particles formed by aggregation, and evaporated at the base of the cloud. N_0^* is then of the order of that in stratiform rain, i.e. 10^6 to 10^7 m^{-4}. In both cases the same low reflectivity corresponds to quite a different equivalent rain rate. The Snow Profiling Algorithm (SPA) mainly applies to stratiform precipitation, and aims at retrieving the N_0^* parameter needed to perform an accurate retrieval of the solid precipitation rate, by taking into account the *aggregation process*. The latter occurs when two ice particles encounter due two their differential sedimentation velocity, inducing a decrease of the particle concentration from the top of the ice cloud to the freezing level.

Correspondence to: E. Moreau
(emmanuel.moreau@novimet.fr)

2 Aggregation model of SPA

The kernel of SPA lies on the fact that each change in n_T results from a collision between particles. Such a collision occurs because of the differential sedimentation velocity between particles, due to the variability of particle diameters. In this model, the terminal velocity of each diameter is related to its density through the formulation of Mitchell (1996). Integrating such differential velocity in the sample volume gives rise to the collision frequency, using a relationship between the cross-sectional area of the particle and its equivalent melted diameter D_{eq}.

Because aggregation may result from a proportion of collisions only, an efficiency coefficient (denoted k_{eff}) is applied, set to 0.3 in a first approximation.

The input of the model is the profile of measured reflectivity factor Z. This information is ingested in the model through a relationship between Z/N_0^* and D_m. In the Rayleigh domain, in which Z is associated with the 6th moment (M_6) of the particle size distribution (as a function of D_{eq}) this relationship is straightforward, consisting in a simple power-law:

$$Z/N_0^* \quad \propto \; D_m^7 \tag{1}$$

Moreover, additional assumptions are required:

(i) the intrinsic shape of the PSD: Delanoë et al. (2004) have shown from an extensive data set that the best fit for intrinsic shape of ice PSD was an exponential function of D_{eq}:

$$N(D_{eq}) = N_0^* \exp(-4D_{eq}/D_m) \tag{2}$$

(ii) the density-size relationship, expressed as a power law:

$$\rho = \rho_0 D^\gamma \tag{3}$$

Note that such a law may be tuned. However, the one used as default is given by Brown and Francis (1995), with γ=−1.1 and ρ(100 μm)=0.92 g.cm^{-3}.

3 Observations

Vertical profiles of reflectivity collected by the McGill University UHF radar (Montreal, Canada) have been used for illustrating SPA algorithm. The cases studied were selected for the thickness of the observed ice layer, and for their stratiform character.

Note that in UHF band (∼900 MHz), the Rayleigh approximation applies in the whole range of particle diameters in ice and snow layers.

Top panel of Fig. 1 displays the vertical reflectivity profiles measured on April 22, 2000, showing a typical stratiform case from 03:00 pm to 00:00 am , with a noticeable bright band observed between 0.5 km and 0.9 km altitude.

N_o^*- and D_m-vertical profiles output from SPA are displayed in the middle and bottom panels respectively.

N_o^* parameter vertically decreases from the cloud top to the freezing level by a factor of 100 or 1000, depending on the situation. Inversely, and as expected when aggregation occurs, the volume equivalent melted diameter D_m increases from the top to the bottom of the ice cloud. Note that the growth of particle size strongly depends on the gradient of the reflectivity.

4 Comparison with POSS data

For comparison, data obtained from a collocated POSS (Precipitation Occurrence Sensor System) have been used, providing drop size distributions for rain precipitation. Details of the treatment are described by Shepard (1990).

The April 22, 2000 is particularly suitable for this comparison, since the bright band altitude is quite low (about 0.5 km altitude), allowing to consider that rain measured at the ground are close to the rain occurring just beneath the bright band.

Figure 2 compares D_m, N_o^* and R time evolution from the following:

1. drop size distribution measured by the POSS at the ground surface in rain layer;
2. SPA output (using the UHF measurements), at the freezing level, i.e. at the top of the bright band.

For both kind of data, a temporal filtering is employed to collocate in time the two instruments. The temporal filtering consists in a smooth according to 10-min wide bell-shaped weighting function.

This comparison shows a general good agreement both in terms of the time variations and absolute values of the D_m and R parameters. The larger N_o^* in the ice than in the rain can be explained by the difference between the terminal fall speed of the solid and the liquid particles. The D_m defined as the equivalent melted particle diameter (same as for R) is directly comparable with the POSS measurements, assuming a conservation of the precipitation flux in the rain layer.

In terms of precipitation rate, the time/amplitude evolution is well described by SPA, with a maximum value of 2 mm/h around 20 h, and is in very good agreement with the observations. On this meteorological case, a "classical" Z-R relationship (Z=200$R^{1.5}$) applied to UHF-reflectivity at the surface gives similar results, excepted at 20 h with to large rain rates.

5 Conclusions and discussion

Results obtained from UHF data seem very promising, since the comparisons with POSS data show a general good agreement both in terms of time variations and of absolute values of the retrieved parameters. Obviously, more cases need to be studied to confirm such a result in a statistical way.

However, the application of SPA illustrated in this paper may be improved from several points of view:

- One must be aware that the lagrangian evolution of n_T had been simplified by assuming a steady state and neglecting horizontal gradients, thus considering vertical gradients only. Next improvements will take into account the slant trajectories of falling particles.
- More realistic model should consider an efficiency coefficient k_{eff} decreasing with altitude (personal communication from Dr. Isztar Zawadzki), with a maximum value set to 0.3 at the freezing level.
- The density model used in the model may be adjusted in some cases. The density model derived from Brown and Francis (1995) is generally satisfying, but it seems to be insufficiently suitable for some few cases studied (not shown).

Acknowledgements. We wish to thank Dr. Gyu Won. Lee from McGill University who kindly provided the UHF radar data as well as the POSS data.

References

Brown, P. and Francis, P.: Improved measurements of ice water content in cirrus using a total water probe, J. Atmos. Oceanic Technol., 12, 410–414, 1995.

Delanoë, J., Protat, A., Testud, J., and Bouniol, D.: Statistical properties of normalized ice particle size distributions from in-situ microphysical measurements. Part I: Stability of the shape of the normalized distribution, J. Appl. Meteor., submitted, 2004.

Field, P. R. and Heymsfield, A. J.: Aggregation and scaling of ice crystal size distributions, J. Atmos. Sci., 60, 544–560, 2003.

Mitchell, D. L.: Use of mass and area dimensional power laws for determining precipitation particle terminal velocities., J. Atmos. Sci., 51, 797–816, 1996.

Pruppacher, H. R. and Klett, R. L.: Microphysics of clouds and precipitations, Reidel Publishing Compagny, pp. 714, 1978.

Sheppard, B. E.: Measurement of raindrop size distributions using a small Doppler radar, J. Atmos. Oceanic Technol., 7, 255–268, 1990.

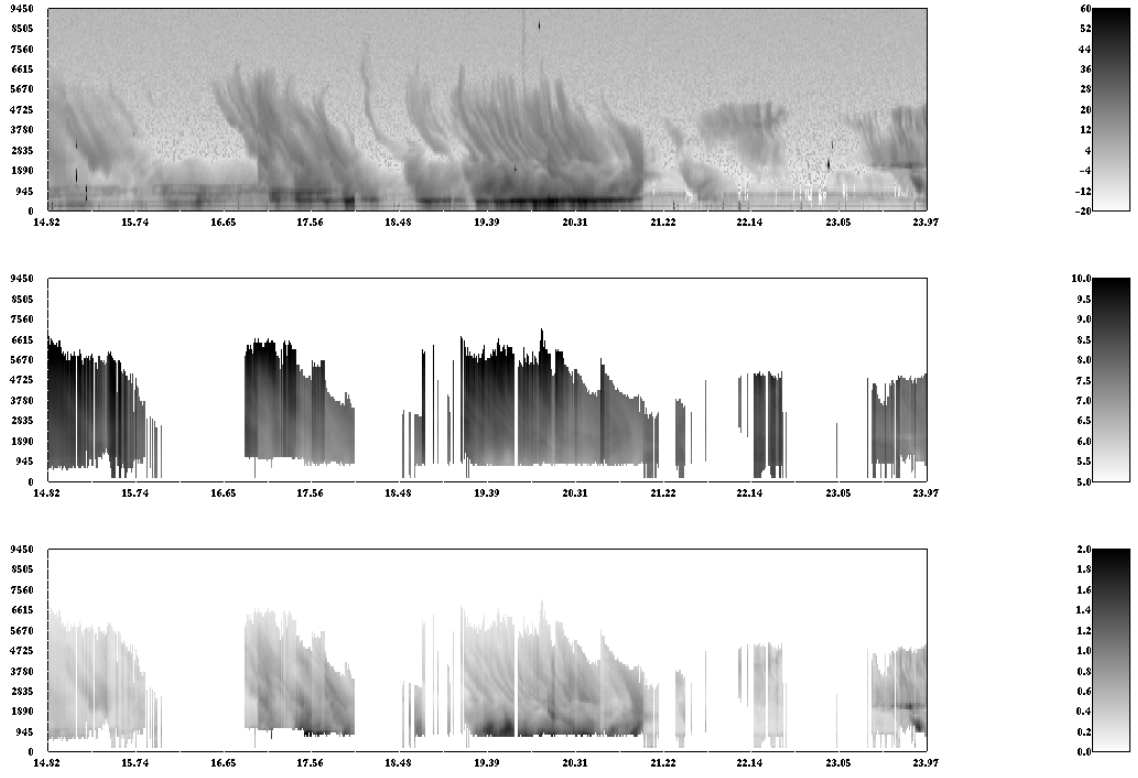

Fig. 1. Vertical profiles of reflectivity (in dBZ) measured by the UHF radar (top panel), retrieved No* profiles (middle panel) and retrieved D_m profiles (bottom panel), 22 April 2000, McGill, CANADA.

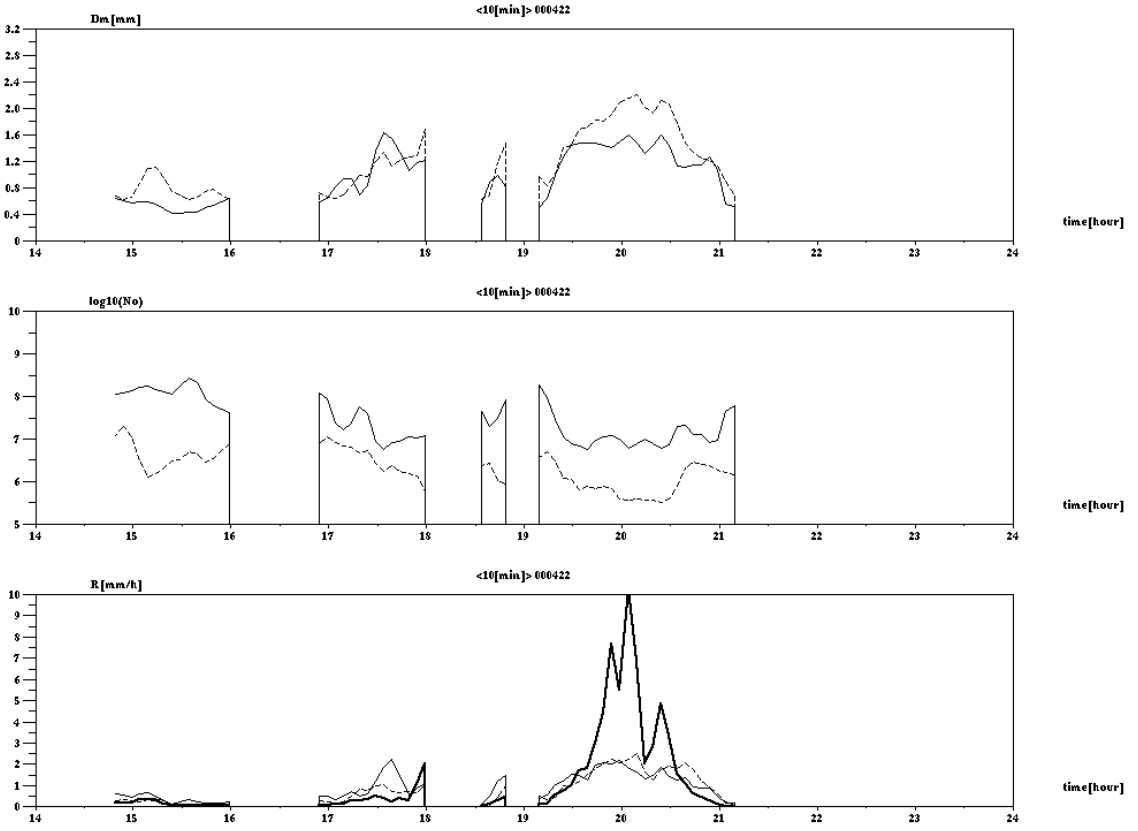

Fig. 2. Time series of 10 min averaging D_m, No* and snow rate R retrieved from SPA at 0°Celsius (solid line) and measurements from POSS at the surface (dashed line). The bold solid line corresponds to the "standard relation" $Z=200R^{1.5}$, 22/04/2000, McGill, CANADA.